PERGAMON

International Journal of Heat and Mass Transfer 42 (1999) 1585–1595

International Journal of HEAT and MASS TRANSFER

# Turbulence phenomena in the radio frequency induction plasma torch

Rubin Ye, Pierre Proulx, Maher I. Boulos*

*Plasma Technology Research Center (CRTP), Department of Chemical Engineering, University of Sherbrooke, Sherbrooke, Quebec, Canada J1K 2R1*

Received 22 January 1998; in final form 6 August 1998

**Abstract**

The mathematical modeling of the flow and temperature fields in an inductively coupled radio frequency (rf) plasma torch is carried out with the objective of elucidating the basic of turbulence phenomena met under such discharge conditions. Temperature and density fluctuations are included in the $k$–$\varepsilon$ turbulence model to investigate their effect on the plasma turbulence and energy transfer. Two distinct regions, one almost fully laminar and another significantly turbulent, are shown to coexist in the discharge. The effects of operation parameters on the plasma turbulence are discussed. 

**Nomenclature**

$a$, $b$ variables for the p.d.f. calculation
$C_p$ specific heat at constant pressure
$C_\mu$, $C_{\varepsilon 1}$, $C_{\varepsilon 2}$, $C_g$, $C_T$ turbulence model constants
f rf frequency
$f$ independent scalar
$f'$ variable for the p.d.f. calculation
$f_{max}$, $f_{min}$ integration limits in the p.d.f. calculation
$\bar{F}_{Lr}$, $\bar{F}_{Lz}$ radial and axial Lorentz force
$G$ generation rate of turbulent kinetic energy
$G_T$ generation rate of temperature variance
$h$ plasma enthalpy
$k$ turbulent kinetic energy
$P_0$ plasma power
$\bar{p}$ pressure
$p(f)$ probability density function (p.d.f.)
$Pr$ Prandtl number
$Q$, $Q_1$, $Q_2$, $Q_3$ plasma gas flow rates
$\bar{Q}_J$ Joule heating rate
$r$ radial coordinate
$R_0$, $R_1$, $R_2$, $R_3$, $R_c$ radial dimensions of the rf plasma torch
$Re_0$, $Re_c$, $Re_s$ Reynolds numbers
$r_{turbint}$ relative turbulence intensity
$r_\mu$ relative turbulent viscosity
$T$ plasma temperature
$T''^2$ temperature variance
$T_{f_{max}}$, $T_{f_{min}}$ upper and low limits of the temperature
$U$ entrance gas velocity
$\bar{U}_R$ volumetric radiation energy loss rate
$u$, $v$, $w$ velocity components in $(z, r, \theta)$ directions
$z$ axial coordinate
$z_1$, $z_2$, $z_3$, $z_p$, $z_s$ axial dimensions of the rf plasma torch.

*Greek symbols*

$\varepsilon$ dissipation rate of turbulent kinetic energy
$\phi$, $\tilde{\phi}$ density-weighted and time-averaged quantities
$\phi_f$ quantity related to scalar $f$
$\kappa$ thermal conductivity
$\Gamma$ transport coefficient
$\mu$ viscosity
$\nu$ kinematic viscosity
$\bar{\rho}$ plasma density
$\rho(f)$ generalized density
$\sigma$ standard deviation.

*Subscripts*

eff effective transport property
l, t laminar and turbulent property
k property relative to turbulent kinetic energy
$\varepsilon$ property relative to dissipation rate of the turbulent kinetic energy.

* Corresponding author. Fax: 001 819 821 7955

0017–9310/98/$ - see front matter 
PII: S0017–9310(98)00260–9

## 1. Introduction

The inductively coupled radio frequency (rf) plasma has found its applications in various fields, especially for the synthesis of new material, preparation of ultra fine powders (UFP) and plasma spraying coating. Mathematical modeling of the momentum, heat and mass transfer has become one of the major techniques in the study of rf plasma. A number of models were proposed for computation of the flow, temperature and concentration fields [1–6]. These models cover both the laminar and turbulent flow conditions. The $k$–$\varepsilon$ fluid model has been used by El-Hage et al. [3] and Chen and Boulos [4] to study the flow and temperature fields in the rf plasma torch. They pointed out that there are two regions in a rf plasma, i.e., the laminar region and the turbulent region. Most recently, Chen et al. [7] and Merkhouf et al. [8] extended the standard $k$–$\varepsilon$ turbulence model to a three-equation (3E) turbulence fluid model by taking into account the density fluctuation in the plasma and presented some preliminary results. However, details of the turbulence phenomena were not evaluated.

Because of the significant influence of the turbulence on the heat and mass transport phenomena in the rf discharge, and the difficulty of obtaining detailed turbulence measurements in the high temperature discharge region, emphasis was placed on the use of mathematical modeling as a means of studying the turbulence behavior in the rf plasma torch. The plasma turbulent viscosity and the turbulence intensity in various plasma flow conditions are calculated. The results provide a valuable insight of the turbulence phenomena in the rf plasma torch.

## 2. The turbulence fluid model

### 2.1. Basic assumptions

(a) Steady state and isotropic turbulent flow;
(b) Axi-symmetric two-dimensional system of coordinates;
(c) Plasma is in local thermodynamic equilibrium (LTE) condition;
(d) The plasma is optically thin and there is no absorption of the radiation energy losses;
(e) The thermodynamic and transport properties have no fluctuation except density;
(f) The viscosity dissipation of the thermal energy is negligible.

### 2.2. Governing equations

Generally, the temperature fluctuations of thermal plasma will cause the density fluctuations. Therefore, the temperature and density fluctuations are included in this model. In the density fluctuation conditions, the density-weighted average method is used to obtain the closed conservation equations for the turbulent flows [9].

Based on the preceding assumptions and the density-weighted method, the so-called three-equation (3E) turbulent fluid model was obtained and used by Chen et al. and Merkhouf et al. [7, 8] for the rf plasma flows. The governing equations for the 3E fluid model are briefly described as follows (in the equations, the dependent variables with a bar denote the conventional time-averaged quantities, others are the density-weighted averaged quantities, see Merkhouf et al. [8]):

(a) Continuity equation

$$\frac{\partial}{\partial z}(\bar{\rho}u)+\frac{1}{r}\frac{\partial}{\partial r}(r\bar{\rho}v)=0 \tag{1}$$

(b) Momentum conservation equations

$$\frac{\partial}{\partial z}(\bar{\rho}uu)+\frac{1}{r}\frac{\partial}{\partial r}(r\bar{\rho}vu)=\frac{\partial}{\partial z}\left(\mu_{\text{eff}}\frac{\partial u}{\partial z}\right)+\frac{1}{r}\frac{\partial}{\partial r}\left(r\mu_{\text{eff}}\frac{\partial u}{\partial r}\right)-\frac{\partial \bar{p}}{\partial z}+\frac{\partial}{\partial z}\left(\mu_{\text{eff}}\frac{\partial u}{\partial z}\right)+\frac{1}{r}\frac{\partial}{\partial r}\left(r\mu_{\text{eff}}\frac{\partial v}{\partial z}\right)+\bar{F}_{Lz} \tag{2}$$

$$\frac{\partial}{\partial z}(\bar{\rho}uw)+\frac{1}{r}\frac{\partial}{\partial r}(r\bar{\rho}vw)=\frac{\partial}{\partial z}\left(\mu_{\text{eff}}\frac{\partial w}{\partial z}\right)+\frac{1}{r}\frac{\partial}{\partial r}\left(r\mu_{\text{eff}}\frac{\partial w}{\partial r}\right)-\frac{w}{r}\left(\bar{\rho}v+\frac{\mu_{\text{eff}}}{r}+\frac{\partial \mu_{\text{eff}}}{\partial r}\right) \tag{4}$$

where $u$, $v$, $w$ are the axial, radial and tangential components of the flow velocity; $\bar{F}_{Lz}$ and $\bar{F}_{Lr}$ are axial and radial components of the Lorentz force; $\mu_{\text{eff}}=\mu_l+\mu_t$ is the effective viscosity of the plasma, which is the sum of the molecular viscosity $\mu_l$ and the turbulent viscosity $\mu_t$.

(c) Energy conservation equation

$$\frac{\partial}{\partial z}(\bar{\rho}uh)+\frac{1}{r}\frac{\partial}{\partial r}(r\bar{\rho}vh)=\frac{\partial}{\partial z}\left(\Gamma_{\text{eff}}\frac{\partial h}{\partial z}\right)+\frac{1}{r}\frac{\partial}{\partial r}\left(r\Gamma_{\text{eff}}\frac{\partial h}{\partial z}\right)+\bar{Q}_J-\bar{U}_R \tag{5}$$

where $h$ is the plasma enthalpy, $\Gamma_{\text{eff}}=(\kappa/C_p)+(\mu_t/Pr_t)$, is the combined molecular and turbulent energy transport coefficient, $Pr_t$ is the turbulent Prandtl number. $\bar{Q}_J$ and $\bar{U}_R$ are the Joule heating rate and the volumetric radiation energy loss rate of the plasma.

(d) $k$–$\varepsilon$ equations

$$\frac{\partial}{\partial z}(\bar{\rho}uk)+\frac{1}{r}\frac{\partial}{\partial r}(r\bar{\rho}vk)=\frac{\partial}{\partial z}\left(\Gamma_{\mathrm{k}}\frac{\partial k}{\partial z}\right)+\frac{1}{r}\frac{\partial}{\partial r}\left(r\Gamma_{\mathrm{k}}\frac{\partial k}{\partial r}\right)+G-\bar{\rho}\varepsilon \quad (6)$$

$$\frac{\partial}{\partial z}(\bar{\rho}u\varepsilon)+\frac{1}{r}\frac{\partial}{\partial r}(r\bar{\rho}v\varepsilon)=\frac{\partial}{\partial z}\left(\Gamma_{\varepsilon}\frac{\partial \varepsilon}{\partial z}\right)+\frac{1}{r}\frac{\partial}{\partial r}\left(r\Gamma_{\varepsilon}\frac{\partial \varepsilon}{\partial r}\right)+C_{\varepsilon 1}G\frac{\varepsilon}{k}-C_{\varepsilon 2}\bar{\rho}\frac{\varepsilon^2}{k} \quad (7)$$

where $\Gamma_{\mathrm{k}}=\mu_{\mathrm{l}}+(\mu_{\mathrm{t}}/Pr_{\mathrm{k}})$, $\Gamma_{\varepsilon}=\mu_{\mathrm{l}}+(\mu_{\mathrm{t}}/Pr_{\varepsilon})$, are the combined transport coefficients for the turbulent kinetic energy $k$ and its dissipation rate $\varepsilon$, respectively, $\mu_{\mathrm{T}}=\bar{\rho}C_{\mu}k^2/\varepsilon$; $Pr_{\mathrm{k}}$ and $Pr_{\varepsilon}$ are the corresponding Prandtl numbers. $G$ is the generation rate of the turbulent kinetic energy,

$$G=\mu_{\mathrm{t}}\left\{2\left[\left(\frac{\partial u}{\partial z}\right)^2+\left(\frac{\partial v}{\partial r}\right)^2+\left(\frac{v}{r}\right)^2\right]+\left(\frac{\partial w}{\partial z}\right)^2+\left[r\frac{\partial}{\partial r}\left(\frac{w}{r}\right)\right]^2+\left(\frac{\partial u}{\partial r}+\frac{\partial v}{\partial z}\right)^2\right\} \quad (8)$$

(e) Temperature variance equation

$$\frac{\partial}{\partial z}(\bar{\rho}uT''^2)+\frac{1}{r}\frac{\partial}{\partial r}(r\bar{\rho}vT''^2)=\frac{\partial}{\partial z}\left(\Gamma_{\mathrm{eff}}\frac{\partial T''^2}{\partial z}\right)+\frac{1}{r}\frac{\partial}{\partial r}\left(r\Gamma_{\mathrm{eff}}\frac{\partial T''^2}{\partial r}\right)+C_{\mathrm{g}}G_T-C_T\bar{\rho}\left(\frac{\varepsilon}{k}\right)T''^2 \quad (9)$$

where

$$G_T=\frac{\mu_{\mathrm{t}}}{Pr_{\mathrm{t}}}\left[\left(\frac{\partial T}{\partial z}\right)^2+\left(\frac{\partial T}{\partial r}\right)^2\right] \quad (10)$$

is the generation rate for the temperature variance.

The constants in the preceding equations (1)–(10) are as follows:

$C_{\mu}=0.9, C_{\varepsilon 1}=1.44, C_{\varepsilon 2}=1.92, C_{\mathrm{g}}=2.0,$

$C_T=6.0, Pr_{\mathrm{k}}=1.0, Pr_{\varepsilon}=1.30, Pr_{\mathrm{t}}=0.7.$

### 2.3. The influence of temperature fluctuations on the density

At the density fluctuation conditions, the time-averaged density can be obtained by introducing a suitable probability density function (p.d.f.) $p(f)$. The p.d.f. to be constructed is a density-weighted function, which allows the evaluation of both density-weighted and time-averaged values. The density-weighted averaged values are given by

$$\phi=\int_0^1 \phi_f p(f)\,\mathrm{d}f \quad (11)$$

and the time-averaged values are given by

$$\bar{\phi}=\bar{\rho}\int_0^1 \frac{\phi_f}{\rho(f)}p(f)\,\mathrm{d}f \quad (12)$$

The time-averaged density can be obtained by

$$\bar{\rho}=\left[\int_0^1 \frac{p(f)}{\rho(f)}\,\mathrm{d}f\right]^{-1} \quad (13)$$

where $\phi_f$ stands for any quantity which may be uniquely related to the scalar $f$, including the temperature, velocity and concentration, etc. [10, 11]. The above definitions of density-weighted average and time average by using a p.d.f. and the conventional definitions through ensemble average are identical.

In thermal plasma, density fluctuations usually arise from the temperature fluctuations. Therefore, it is better to associate the p.d.f. with the temperature fluctuations. Furthermore, we assume the density fluctuations are uniquely caused by that of the temperature. The p.d.f. suggested by Lee and Pfender [12] is used in the calculation:

$$p(f)=\frac{f^{a-1}(1-f)^{b-1}}{\int_{f_{\min}}^{f_{\max}} f^{a-1}(1-f)^{b-1}\,\mathrm{d}f};\quad f_{\min}<f<f_{\max} \quad (14)$$

with

$$\int_{f_{\min}}^{f_{\max}} p(f)\,\mathrm{d}f=1.$$

The temperature variance is chosen to be the scalar in this study. The variables in equation (14) are defined as

$$a=f\left[\frac{f(1-f)}{f'}\right],\quad b=\frac{1-f}{f}a,\quad f=\frac{T_f}{T_{f_{\max}}},\quad f'=\frac{T''^2}{T_{f_{\max}}^2},$$

$$T_{f_{\max}}=T+3\sqrt{T''^2},\quad T_{f_{\min}}=T-3\sqrt{T''^2}$$

The temperature dependence of $T_f$ is assumed to follow the $\beta$-probability distribution with a standard deviation of $\sigma=\sqrt{T''^2}$ and mean temperature $T$.

Table 1
Dimensions and operation parameters of the rf plasma torch

| | |
|---|---|
| $R_1=1.35$ mm | $z_1=35.15$ mm |
| $R_2=4.80$ mm | $z_2=75.15$ mm |
| $R_3=13.0$ mm | $z_3=113.0$ mm |
| $R_0=17.5$ mm | $z_{\mathrm{p}}=60.0$ mm |
| $R_{\mathrm{C}}=22.0$ mm | $z_{\mathrm{s}}=35.15$ mm |
| $Q_1=10$ slpm† (Ar) | $P_0=15$–$30$ kW |
| $Q_2=25$ slpm† (Ar) | $f=3$ MHz |
| $Q_3=40$–$80$ slpm† (90%Ar+10%$H_2$,vol) | $p=26.7$–$101.3$ kPa |

† slpm-standard liter per minute

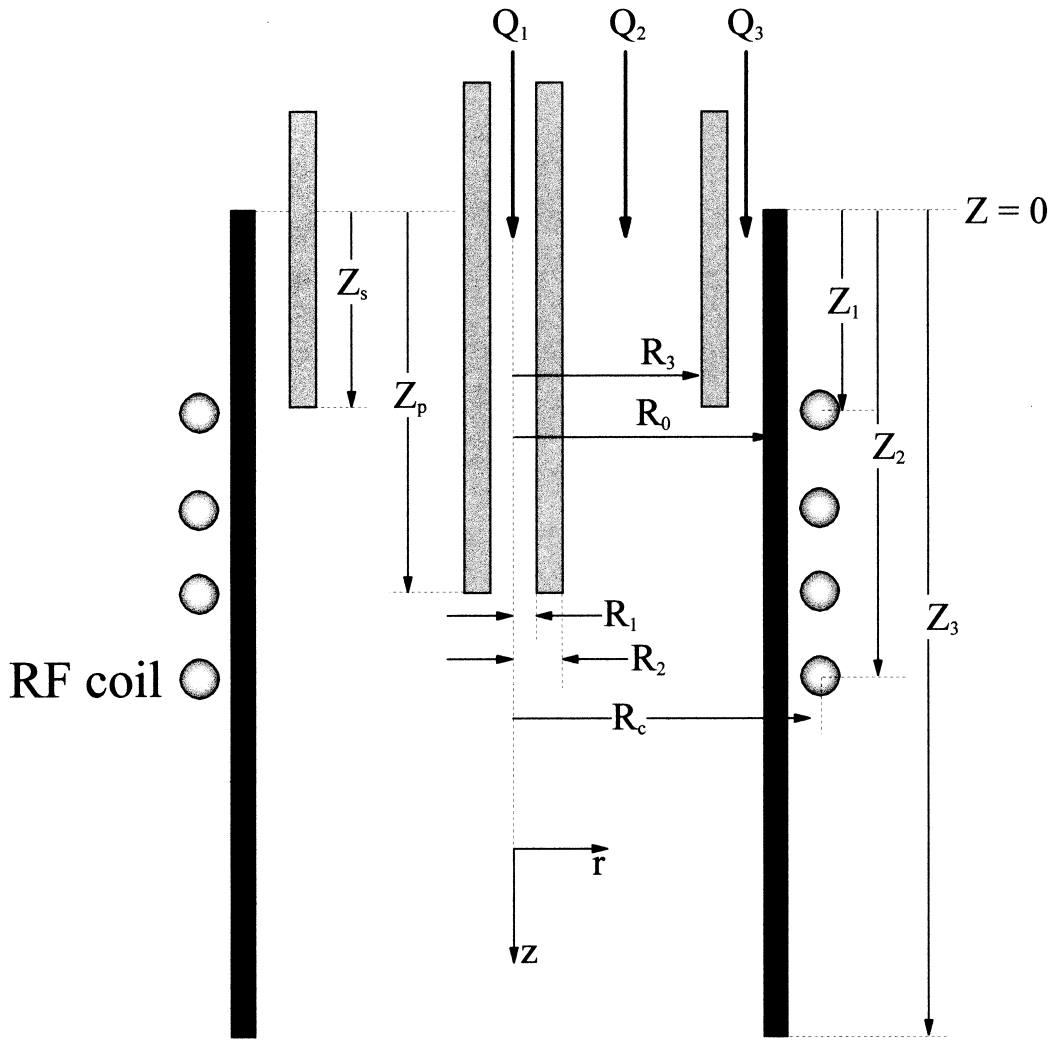


Fig. 1. The geometry and coordinates of the rf inductively coupled plasma torch.

## 3. Torch geometry and operation conditions

The rf plasma torch and the corresponding coordinates used in the present study are schematically shown in Fig. 1. Table 1 summarizes the main torch dimensions and operation parameters. In order to obtain a satisfactory cooling of the inner torch wall, a sheath tube $r = R_3$ is inserted into the torch, the sheath gas $Q_3$ is injected into the torch by passing through the annular channel between the sheath tube and the inner torch wall. Because the flow rate of the sheath gas is relatively high, it could be an important source of plasma turbulence. A volumetric percentage of 10% hydrogen is added to the argon sheath gas.

## 4. Results and discussion

The conservation equations of the 3E turbulent fluid model were solved by using the same boundary conditions as used by Merkhouf et al. [8]. The calculations domain for the rf plasma torch is $z$: 0–113.0 mm, $r$: 0–17.5 mm; with a non-uniform grid of $39 \times 35$ mesh points. The program is based on the SIMPLER method, which was introduced by Patankar [13]. A convergence criteria of the maximum relative error of any dependent variables is less than $5 \times 10^{-4}$ was used in the calculation. The results are presented in terms of the isocontours of the plasma temperature, flow field as well as those of the relative turbulence intensity and the ratio of the turbulent to

the laminar viscosity. The latter were calculated as follows:

(a) Relative turbulence intensity

$$r_{\text{turbint}} = \frac{\sqrt{2k/3}}{\sqrt{u^2+v^2+w^2}} \tag{15}$$

(b) Relative turbulent viscosity

$$r_{\mu} = \frac{\mu_{\text{t}}}{\mu_{\text{l}}} \tag{16}$$

### 4.1. The general behavior of the turbulence in the rf plasma torch

As mentioned earlier in Section 2.3, the density variations due to temperature fluctuations of the plasma flow is taken into account in the present model. Figure 2(a) and (b) show the temperature fields in the rf plasma torch obtained by the standard $k$–$\varepsilon$ model and the present three-equation model, respectively. Computations were carried out for a plasma torch at a power level of 15 kW, $Q_3 = 80$ slpm and at atmospheric pressure conditions. The corresponding relative turbulent viscosity fields are shown in Fig. 3(a) and (b). No significant difference is observed in the calculated temperature and relative viscosity fields. Radial profiles of the temperature and relative turbulent viscosity, at $z = 86$ mm, obtained using the standard $k$–$\varepsilon$ model and the present model, are shown in Fig. 4(a) and (b). These show only small differences at the plasma fringe between the density-weighted averaged temperature and the corresponding time averaged value. We conclude in the present case that the temperature and density fluctuations have a negligible effect on the rf plasma turbulence and energy transfer.

A frequently asked question is what is the important region of the turbulence and what is its magnitude in an rf plasma torch. Generally, we may imagine that the significant region is near the torch wall. It is found from Fig. 3 that there are two major important regions for the plasma turbulence: one is in the downstream and near wall region, where the turbulence is caused by the shear force with the torch wall; another is in the upstream

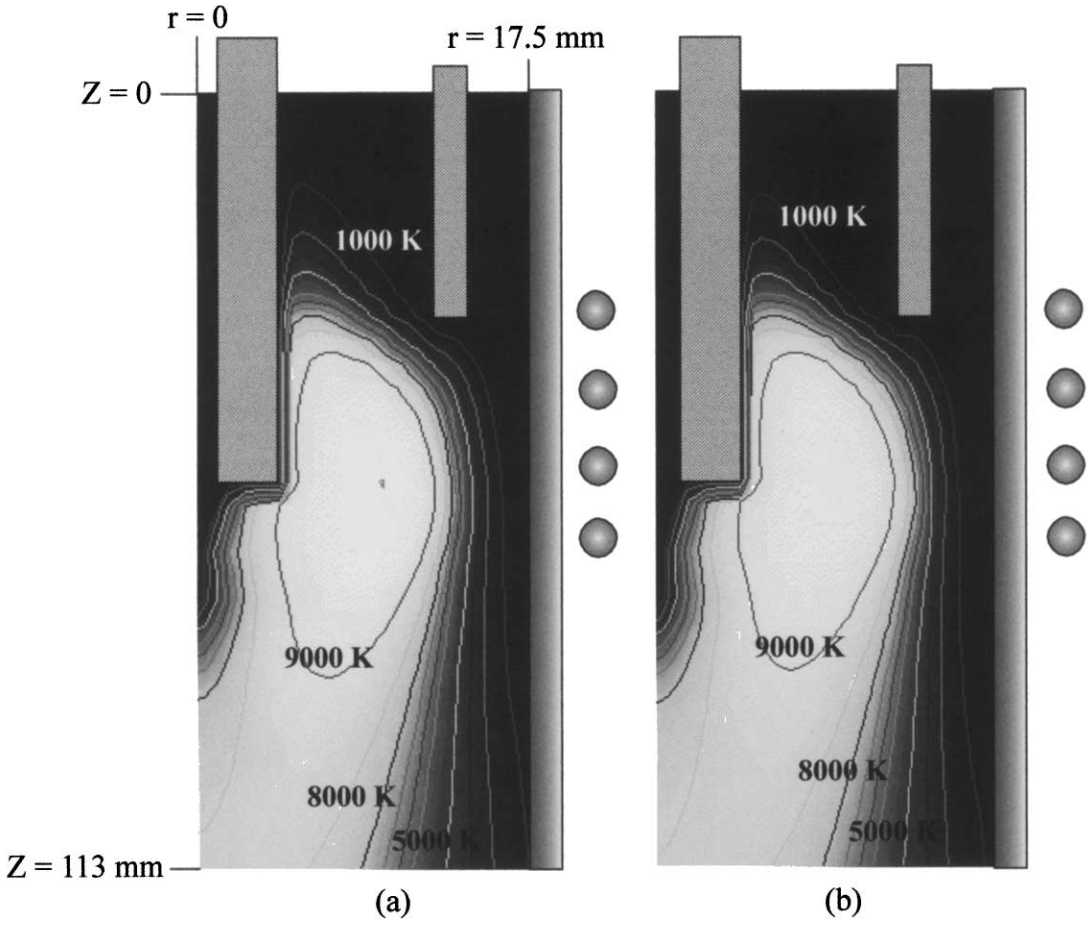


Fig. 2. Temperature fields in the rf plasma torch at 15 kW and atmospheric pressure, (a) standard $k$–$\varepsilon$ model, (b) three-equation model.

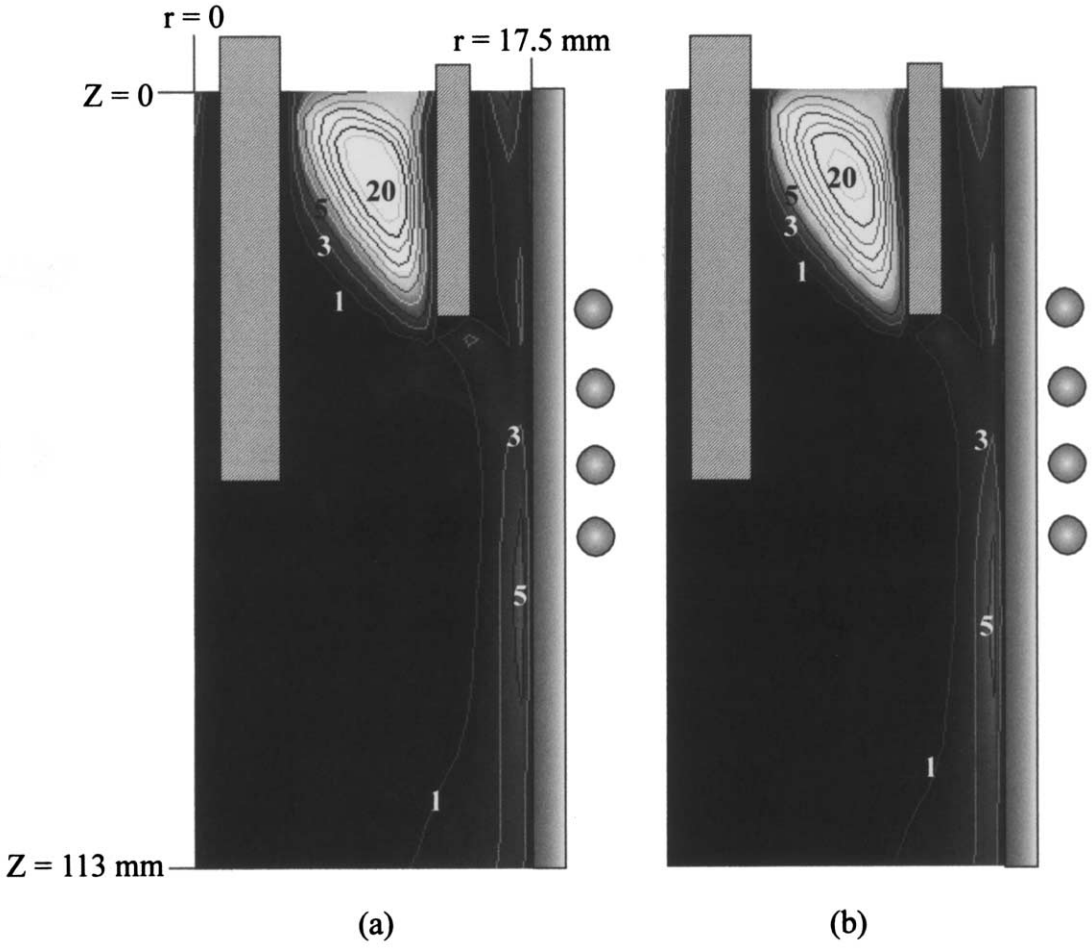


Fig. 3. Relative turbulent viscosity fields in the rf plasma torch at 15 kW and atmospheric pressure, (a) standard $k$–$\varepsilon$ model, (b) three-equation model.

region where the injection cold gas $Q_2$ meets the recirculating high temperature plasma gas, forming a shear layer between the plasma and the injected cold gas. The relative turbulent viscosity of the second region is much greater than that of the first one. It can reach a value of 20 or more. Comparing Figs 2 and 3, we note that a negligible level of turbulence at temperatures over 5000 K.

As a whole, there are two distinct regions in an rf plasma torch. The central high temperature region is dominated by the laminar flow; whereas the near wall and upstream regions are dominated by turbulent flow. Especially in the upstream region, the turbulent effect is so high that the molecular viscosity is almost negligible.

### 4.2. The effect of gas flow rate

In order to form turbulent flows, the working gas are assumed to be injected into the rf plasma torch at two gas flow rates: 75 slpm ($Q_3 = 40$ slpm), 115 slpm ($Q_3 = 80$ slpm). To highlight the effect of gas flow rate, we represent the gas flow rate by the corresponding Reynolds numbers. The Reynolds numbers for the central tube and the torch is

$$Re = \frac{2RU}{v} = \frac{2Q}{\pi v R} \tag{17}$$

where $U$ is the gas velocity at the torch entrance, $Q$ is the gas flow rate and $v$ is the kinematic viscosity of the gas, respectively, $R$ is the characteristic radius. For the sheath annulus, the Reynolds number is calculated by the formula proposed by Bird et al. [14]

$$Re_s = \frac{2(R_0 - R_3)U}{v} = \frac{2Q_3}{\pi v(R_0 + R_3)} \tag{18}$$

Accordingly, the Reynolds numbers at the entrances for different flow conditions are:

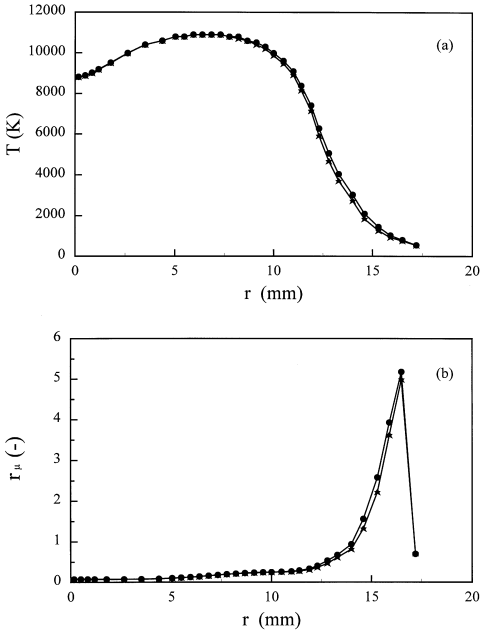


Fig. 4. Radial profiles of plasma temperature (a) and relative turbulent viscosity (b), $z = 86$ mm, o—standard $k$–$\varepsilon$ model, ×—three-equation model.

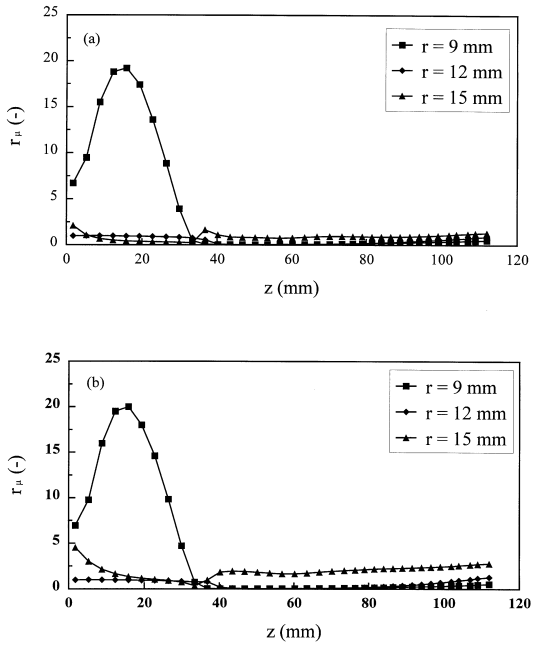


Fig. 5. Axial profiles of the relative turbulent viscosity at $P_0 = 15$ kW at atmospheric pressure, (a) $Q_3 = 40$ slpm, (b) $Q_3 = 80$ slpm.

| | $Q_3 = 40$ slpm | $Q_3 = 80$ slpm |
|---|---|---|
| Torch Reynolds number $Re_0$ | 3387 | 5195 |
| Central tube Reynolds number $Re_c$ | 5856 | 5856 |
| Sheath annulus Reynolds number $Re_s$ | 1037 | 2074 |

The axial profiles of the relative turbulent viscosity for $Q_3 = 40$ slpm and $Q_3 = 80$ slpm at three radial positions: $r = 9$, 12 and 15 mm, are shown in Fig. 5(a) and (b). We find that the turbulent viscosity at the upstream is very large, whereas it is small and uniform at the downstream of the plasma. Figure 6(a) and (b) shows the radial profiles of the relative turbulent viscosity at the same conditions as in Fig. 5, at three axial positions: $z = 60$, 86 and 109 mm, respectively. The relative turbulent viscosity is found to be insensitive to the gas flow rate in the downstream and center to mid-center regions; but the turbulent effect (i.e. turbulent viscosity) has an obvious enhancement near the torch wall with the increase of the gas flow rate.

It is interesting to find that, although the Reynolds number of the central gas at the entrance is sufficiently large, the turbulence effect in the central region is negligible. This is because, in the central region, the plasma

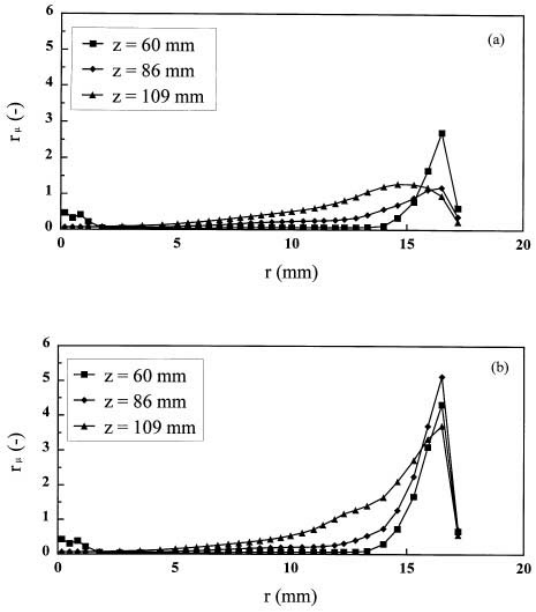


Fig. 6. Radial profiles of the relative turbulent viscosity at $P_0 = 15$ kW and atmospheric pressure, (a) $Q_3 = 40$ slpm, (b) $Q_3 = 80$ slpm.

temperature is very high, therefore, the plasma has a large molecular viscosity, the Reynolds number becomes small.

On the other hand, the turbulence effect becomes significant near the torch wall. This has practical implication in the rf plasma torch. It will reduce the thermal energy loss through the torch wall. Figure 7(a) and (b) show the temperature gradient near the torch wall and the heat flux caused by the conduction thermal energy loss through the wall at different flow conditions, $Q_3 = 40$ and 80 slpm. It is found that, when we increase the gas flow rate, i.e., the plasma becomes more turbulent, the temperature gradient near the torch wall could be significantly decreased, and the energy loss through the torch wall can be reduced greatly.

### 4.3. The effect of pressure

Figure 8(a) and (b) presents the contour plots of the relative turbulent viscosity when the torch is run at atmospheric pressure (101.3 kPa) and low pressure (26.7 kPa), when $Q_3 = 40$ slpm and $P_0 = 15$ kW, respectively. We find that, compared to the atmospheric pressure condition, the relatively important regions of turbulence is blown to the downstream of the plasma. This could also be seen from Fig. 9(a) and (b), the corresponding plots of the relative turbulence intensity at the same conditions. Figure 8 also shows that the area and magnitude of turbulence has been significantly reduced from the high pressure to the low pressure condition.

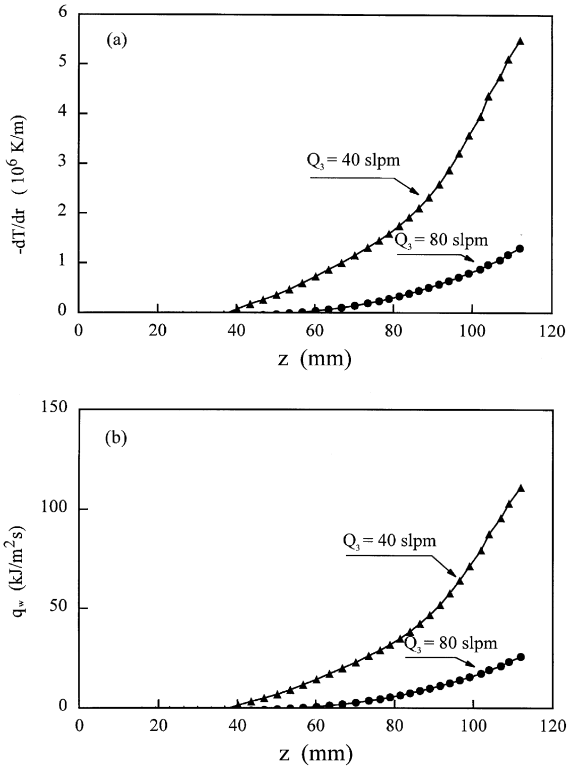


Fig. 7. (a) Temperature gradient near the torch wall, and (b) torch wall heat flux caused by the conduction energy loss at different flow conditions.

### 4.4. The effect of dissipation power

Figure 10 is the axial profiles of the relative turbulent viscosity at $P_0 = 30$ kW. A similar plot is shown in fig. 5(b), where $P_0 = 15$ kW. It shows that the turbulence is decreased at the high power level. This phenomenon is related to the variation of the plasma molecular viscosity with the temperature. The molecular viscosity of an $Ar/H_2$ plasma increases with the temperature when the temperature is less than 10 000 K. By raising the plasma power, the plasma temperature is increased correspondingly. As a result, the molecular plasma viscosity is increased, this causes the decrease of the Reynolds number, and the turbulence becomes less significant.

## 5. Conclusions

In summary, the turbulence phenomena in the rf plasma torch have been studied at the density and temperature fluctuation conditions by using the $k$–$\varepsilon$ turbulence model. The mathematical modeling results show that the density and temperature fluctuations have negligible effect on the rf plasma turbulence and temperature field. Two kinds of significantly different flow regions are found to coexist in the rf plasma. The plasma turbulence, either its intensity or its viscosity, is considerably larger in the near wall and upstream regions of the torch, for example, the relative turbulent viscosity can reach as much as 20 or more. The turbulence effect is negligible in the region with the plasma temperature over 5000 K. The turbulence becomes significant when the gas flow rate is increased. By reducing the operation pressure, the turbulent field will move to the downstream of the torch. The plasma turbulence can be reduced by increasing the dissipation power.

## Acknowledgements

The authors gratefully acknowledge the financial support by the Consil de Recherche en Sciences Naturelles en Génie de Canada (CRSNG) and the Fonds pour la Formation de Chercheurs et l'Aide a la Recherche (FCAR).

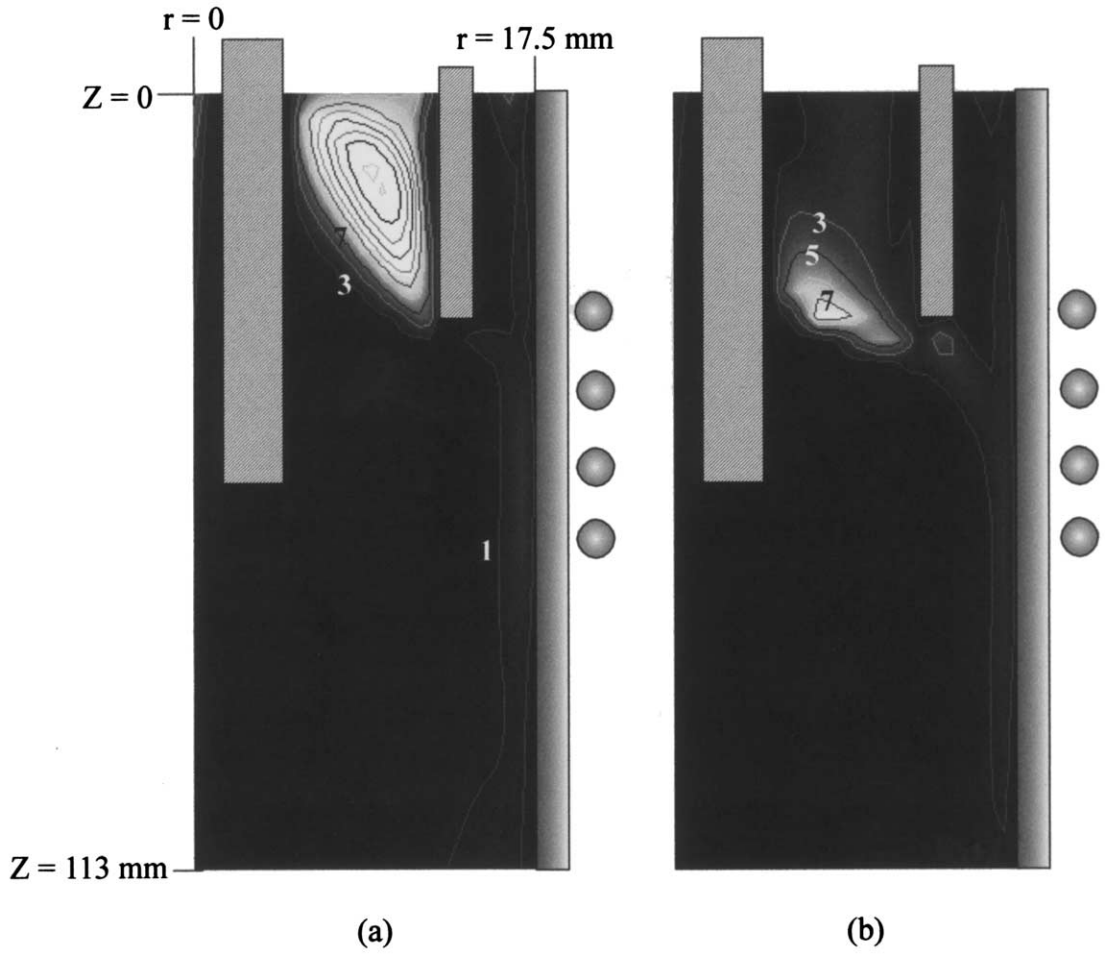


Fig. 8. Contour plots of the relative turbulent viscosity at $P_0 = 15$ kW and $Q_3 = 40$ slpm, (a) pressure = 101.3 kPa, (b) pressure = 26.7 kPa.

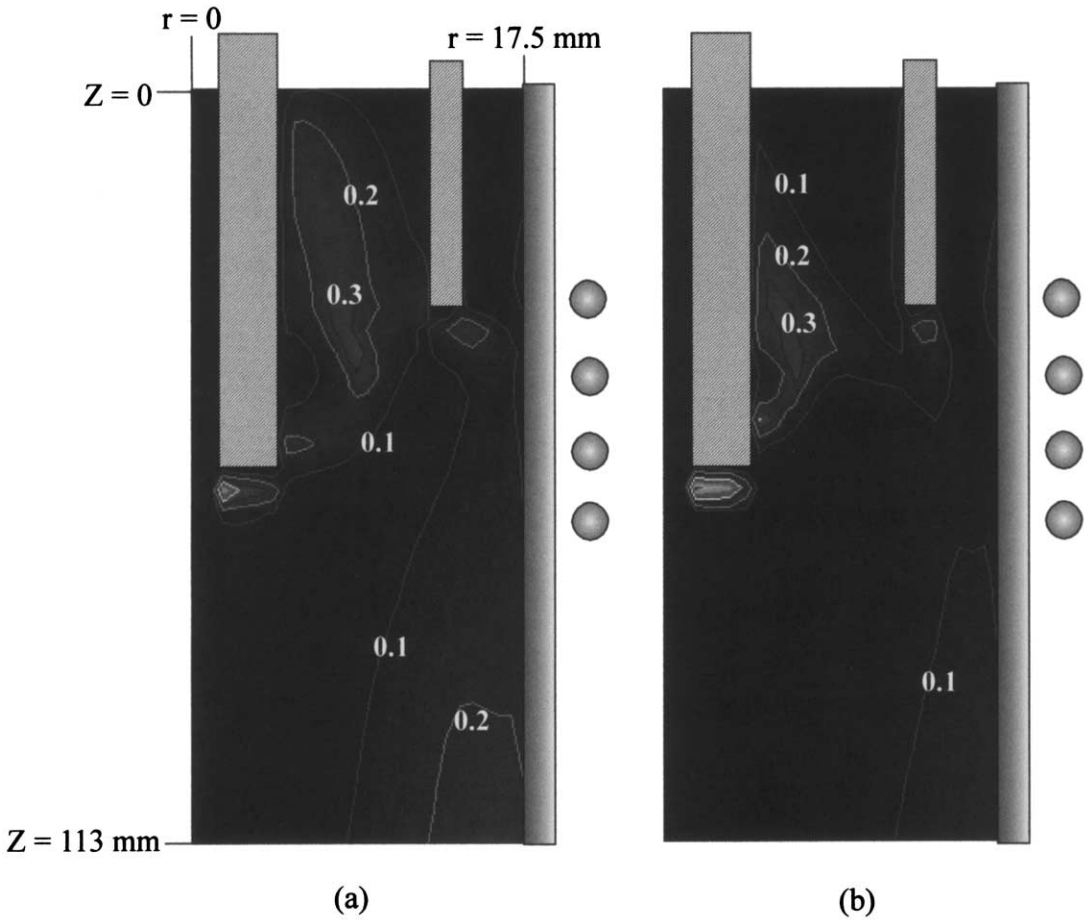


Fig. 9. Contour plots of the relative turbulence intensity at $P_0 = 15$ kW and $Q_3 = 40$ slpm, (a) pressure = 101.3 kPa, (b) pressure = 26.7 kPa.

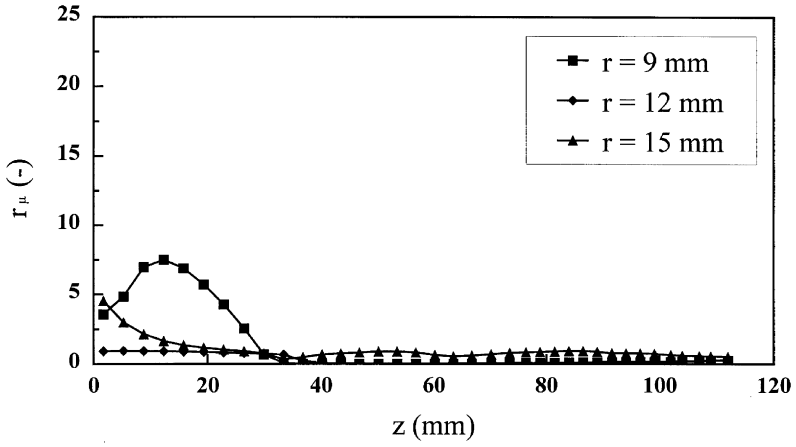


Fig. 10. Axial profiles of relative turbulent viscosity profiles at $P_0 = 30$ kW and $Q_3 = 80$ slpm, atmospheric pressure.

## References


[1] J. Mostaghimi, P. Proulx, M.I. Boulos, Parametric study of the flow and temperature fields in an inductively coupled plasma, Plasma Chem. Plasma Process. 4 (1984) 199–217.

[2] J. Mostaghimi, M.I. Boulos, Two-dimensional electromagnetic fields in induction plasma modeling, Plasma Chem. Plasma Process. 9 (1989) 25–43.

[3] M. El-Hage, J. Mostaghimi, M.I.Boulos, A turbulent flow model for the r.f. inductively coupled plasma, J. Appl. Phys. 65 (1989) 4178–4185.

[4] X. Chen, E. Pfender, Modeling of RF plasma torch with a metallic tube inserted for reactant injection, Plasma Chem. Plasma Process. 11 (1991) 103–128.

[5] M. Rahmane, G. Soucy, M.I. Boulos, Mass transfer in induction plasma reactors, Int. J. Heat Mass Transfer 37 (1994) 2035–2046.

[6] K. Chen, M.I. Boulos, Turbulence in induction plasma modeling, J. Phys. D: Appl. Phys. 27 (1994) 946–952.

[7] X. Chen, A. Merkhouf, M.I. Boulos, Preliminary study of the 3-equation turbulence model of an R.F. Plasma torch, Proceedings of the Third Asia–Pacific Conference on Plasma Science and Technology, vol. 1, Tokyo, Japan, 1996, pp. 71–76.

[8] A. Merkhouf, R. Ye, P. Proulx, M.I. Boulos, Mathematical modeling of plasma systems, Proceedings of The Julian Szekely Memorial Symposium on Materials Processing, Boston, USA, 1997, pp. 509–528.

[9] T. Cebeci, A.M.O. Smith, Analysis of Turbulent Boundary Layers, Academic press, New York, 1974, Chapter 2.

[10] W.P. Jones, J.H. Whitelaw, Calculation methods for reacting turbulent flows: a review, Combustion and Flames 48 (1982) 1–26.

[11] W.P. Jones, Modeling for turbulent flows with variable density and combustion, Prediction Methods for Turbulent Flow, Hemisphere, new York, 1980, p. 379.

[12] Y.C. Lee, E. Pfender, Particle dynamics and particle heat and mass transfer in thermal plasma: thermal plasma jet reactors and multiparticle injection, Plasma Chem. Plasma Process 7 (1987) 1–27.

[13] S.V. Patankar, Numerical Heat Transfer and Fluid Flow, McGraw-Hill, New York, 1980.

[14] R.B. Bird, W.E. Stewart, E.N. Lightfoot, Transport Phenomena, John Wiley and Sons, New York, 1960, p.54.